

THE DISTRIBUTION OF DARK MATTER IN A RINGED GALAXY

A. C. QUILLEN^{1,2} AND J. A. FROGEL^{2,3,4}

Received 1996 August 2; accepted 1997 May 9

ABSTRACT

Outer rings are located at the greatest distance from the galaxy center of any feature resonant with a bar. Because of their large scale, their morphology is sensitive to the distribution of the dark matter in the galaxy. We introduce here how study of these rings can constrain the mass-to-light ratio of the bar, and so the percentage of dark matter in the center of these galaxies.

We compare periodic orbits integrated in the ringed galaxy NGC 6782 near the outer Lindblad resonance to the shape of the outer ring. The nonaxisymmetric component of the potential resulting from the bar is derived from a near-infrared image of the galaxy. The axisymmetric component is derived assuming a flat rotation curve. We find that the pinched non-self-intersecting, periodic orbits are more elongated for higher bar mass-to-light ratios and faster bars. The inferred mass-to-light ratio of the bar depends on the assumed inclination of the galaxy. With an assumed galaxy inclination of $i = 41^\circ$, for the orbits to be consistent with the observed ring morphology, the mass-to-light ratio of the bar must be high, greater than 70% of a maximal disk value. For $i = 45^\circ$, the mass-to-light ratio of the bar is $75\% \pm 15\%$ of the maximal disk value.

Since the velocity field of these rings can be used to constrain the galaxy inclination as well as the periodic orbit that is represented in the ring, further study will yield tighter constraints on the mass-to-light ratio of the bar. If a near-maximal disk value for the bar is required, then there would either be little dark matter within the bar or the dark matter contained in the disk of the galaxy would be non-axisymmetric and would rotate with the bar.

Subject headings: dark matter — galaxies: halos — galaxies: kinematics and dynamics — galaxies: spiral — galaxies: structure

1. INTRODUCTION

Outer rings are located at the greatest distance from the galaxy center of any feature resonant with a bar. Because of their great distance from the galaxy center, their morphology should be sensitive to the distribution of the dark matter in the galaxy. Since they are resonant with the bar, they are also sensitive to the mass-to-light ratio of the bar. These rings provide a unique opportunity to constrain the mass-to-light ratio of the luminous stellar matter in a galaxy, thus providing us with information about the dark matter distribution. Although the morphology of outer rings has been used to constrain bar pattern speeds (Byrd et al. 1994), it has not yet been used to constrain the dark matter distribution.

Disk mass-to-light ratios have been almost exclusively measured by axisymmetric fits to observed rotation curves (see, e.g., Kent 1987a, 1987b; Broeils & Courteau 1997; Begeman, Broeils, & Sanders 1991; Sackett 1997b), which are commonly performed by requiring the disk to be as massive as possible, as in the “maximal disk” model. Disk mass-to-light ratios determined in this manner are model dependent (see Sackett 1997a) and are affected by a variety of assumptions, such as the dark matter halo profile assumed and the bulge/disk decomposition method. In this paper, by measuring the gravitational force of a non-

axisymmetric component, the bar (which is necessarily a disk component), we can constrain the disk mass-to-light ratio in a way that is independent of the radial distribution of the dark matter and does not require the assumption (of the maximal disk model) that the disk is as massive as possible within the limits set by the rotation curve.

Three classes of rings can be seen in normal barred galaxies: nuclear rings located inside the bar; inner rings that envelop the bar; and outer rings that surround the bar. The simulations of Schwarz (1981) first demonstrated that outer rings develop in the ISM near the outer Lindblad resonance of the bar. Outer rings are classified (following Buta & Crocker 1991) as R1-type or R2-type rings, where R1-type rings resemble an oval with dimples at the points where the ring is closest to the bar and R2-type rings are oval and aligned parallel to the bar. When the rings contain spiral structure, they are classified as pseudorings and are denoted R1' or R2' rings. The two types of rings have morphology closed related to the two families of closed orbits near the outer Lindblad resonance (see, e.g., Contopoulos & Grosbøl 1989; Kalnajs 1991). The bar in these galaxies causes many stellar orbits in the plane of the galaxy to intersect themselves. Because gas can shock, it cannot remain in these orbits, so it collects in orbits that are near the periodic orbit families that are not self-intersecting (Schwarz 1981). For an excellent review on the properties of ringed galaxies, see Buta & Combes (1996).

In this paper, we examine the sensitivity of the ring shape of an R1' ringed galaxy to the mass-to-light ratio of the bar. The nonaxisymmetric component of the gravitational potential is derived from a *J*-band image of the galaxy. The morphology of the ring is compared to periodic orbits near the outer Lindblad resonance for different bar mass-to-light

¹ University of Arizona, Steward Observatory, Tucson, AZ 85721; aquillen@as.arizona.edu.

² Astronomy Department, Ohio State University, 174 West 18th Avenue, Columbus, OH 43210.

³ Visiting Astronomer at Cerro Tololo Inter-American Observatories.

⁴ Department of Physics, University of Durham, Durham, United Kingdom.

ratios. Using this comparison, we place limits on the mass-to-light ratio of the bar and so on the distribution of the dark matter in the galaxy.

2. THE IMAGES OF NGC 6782

NGC 6782 is the best example of an R1-type ringed galaxy found to date in the survey of ~ 220 galaxies being carried out at the Ohio State University (OSU) (Frogel, Quillen, & Pogge 1996). In a catalog of southern ringed galaxies (Buta 1995), the galaxy is classified as R1'SB(r)0/a. Buta (1995) shows this galaxy as a nice example of an R1' ringed galaxy and demonstrates that the outer ring is prominent in a $B-I$ color map and therefore is quite blue. Byrd et al. (1994) show NGC 6782 as an example of a galaxy that resembles their slow pattern speed simulations. The R1' ring in NGC 6782 has a radius of $\sim 60''$, which corresponds to 15 kpc assuming a distance of 50 Mpc ($H_0 = 75 \text{ km s}^{-1} \text{ Mpc}^{-1}$) to the galaxy.

The galaxy was observed in the near-infrared J , H , and K bands and in the visible B , V , and R bands. These data are a preliminary part of the OSU galaxy survey (Frogel et al. 1996). The goal of the survey is to produce a library of photometrically calibrated images of late-type galaxies from 0.4 to 2.2 μm . For notes on the observation and reduction techniques, see Pogge et al. (1997) or, for individual examples, Quillen, Frogel, & González (1994) and Quillen et al. (1995). All of the images were observed at the Cerro Tololo Inter-American Observatory. The BVR images were observed at the 0.9 m telescope on 1995 October 25 using the Tek No. 2 1024 \times 1024 pixel CCD with a spatial scale of 0.40 pixel $^{-1}$. Total on-source exposure times were 30, 15, and 10 minutes for B , V , and R , respectively. The JHK images were observed at the 1.5 m telescope on 1995 October 31 and 1995 November 2 using the near-infrared camera and multiobject spectrometer (NICMOS 3) 256 \times 256 pixel infrared array with a spatial scale of 1".16 pixel $^{-1}$. Total on-source exposure times were 15 minutes at J and H and 29 minutes at K band. The infrared images were observed during photometric conditions and were calibrated on the Cerro Tololo Inter-American Observatory/Carnegie image tube (CTIO/CIT) system using standard stars listed by B. Carter & V. Meadows (1995, private communication). The optical images were observed during clear but nonphotometric conditions.

Figure 1 shows B - and J -band images of the galaxy and an R/B color map. In the B -band image (Fig. 1a), the classic figure-eight shape of the R1-type ring can be seen. The ring has some spiral structure, which causes the ring to be brighter on its northeast and southwest sides than on its northwest and southeast sides. This means that the ring does not have perfect mirror symmetry about its major axis. The pinches near the bar ends can be more clearly seen in the brighter, northeast and southwest sides of the ring.

3. THE FORM OF THE GRAVITATIONAL POTENTIAL

To integrate orbits in the plane of the galaxy, we require an estimate of the gravitational potential. We assume that the potential in the plane $\Phi(r, \theta)$ is a sum of two components, an axisymmetric one, $\Phi_0(r)$, and a component $\Phi_2(r)$ proportional to $\cos 2\theta$,

$$\Phi(r, \theta) = \Phi_0(r) + \Phi_2(r) \cos(2\theta), \quad (1)$$

where θ is the azimuthal angle in the plane of the galaxy and r is the radius. We take the bar to be aligned along the axis with $\theta = 0$.

3.1. The Axisymmetric Component

The axisymmetric component of the potential should be consistent with the rotation curve of the galaxy at the location of the outer ring. At the location of the outer ring in NGC 6782, dark matter is expected to contribute to the rotation curve. We therefore could not use a potential derived solely from the light distribution as did Quillen et al. (1994) and Quillen (1996b), because these were dynamical studies of bars in the central few kiloparsec of galaxies.

Unfortunately, there is no published rotation curve for NGC 6782. Few ringed galaxies have measured rotation curves at large radii. However, the few that have been observed have rotation curves that are nearly flat. For example, the rotation curve of ESO 509-98 is very flat (Buta, Lewis, & Purcell 1997), and the H I velocity field shows the rotation curve of NGC 3351 (of similar morphological type) to be nearly flat (A. Bosma, private communication). Simulations of outer rings produce more realistically shaped rings in model galaxies with flat rotation curves (Byrd et al. 1994). In our orbit integrations, therefore, for the axisymmetric component of the potential, Φ_0 , we assume a logarithmic form consistent with a flat rotation curve. The component Φ_0 is determined by one parameter, the circular velocity, which we estimate from the Tully-Fisher relation (see below). We include scaling factors in all values that depend upon this velocity, so that when the actual circular velocity is known, these values can be corrected.

Near-infrared images are superior to visible images for dynamical studies because of their reduced sensitivity to extinction from dust and because they are dominated by light from an older, cooler stellar population, which is more evenly distributed dynamically and a better tracer of the stellar mass in the galaxy than the bluer, hotter stars (see, e.g., Frogel 1988; Frogel et al. 1996). We use the J -band image to determine the gravitational potential owing to the luminous stellar component of the galaxy. The J -band image was used because the sky is flatter outside the bar than it is in the H -band image and because it has higher a signal-to-noise ratio than does the K -band image. The color $J - K = 1.0 \pm 0.05$ is constant across the bar, though the bulge of the galaxy ($r < 7''$) is redder with $J - K = 1.06 \pm 0.05$. The height of the rotation curve from the luminous stellar matter (traced in the J band) allows us to define a maximal disk and show that at the ring a significant dark component is needed to have a realistic flat rotation curve.

3.2. Galaxy Inclination

Before the gravitational potential due to luminous stellar matter can be generated from the infrared image, we must correct for the inclination of the galaxy. A statistical study of R1' ringed galaxies found that these rings have observed axis ratios of $q_0 = 0.74 \pm 0.08$ and position angles on the sky with respect to the bar of $\theta_0 = 90^\circ \pm 9^\circ$ (Buta 1995). Buta (1995) found that R1' rings are very nearly perpendicular to the bar and are elongated. Gas simulations of these rings support Buta's finding for the ring alignment (Byrd et al. 1994). We therefore assume that the ring is perpendicular to the bar. This assumption reduces the degrees of freedom

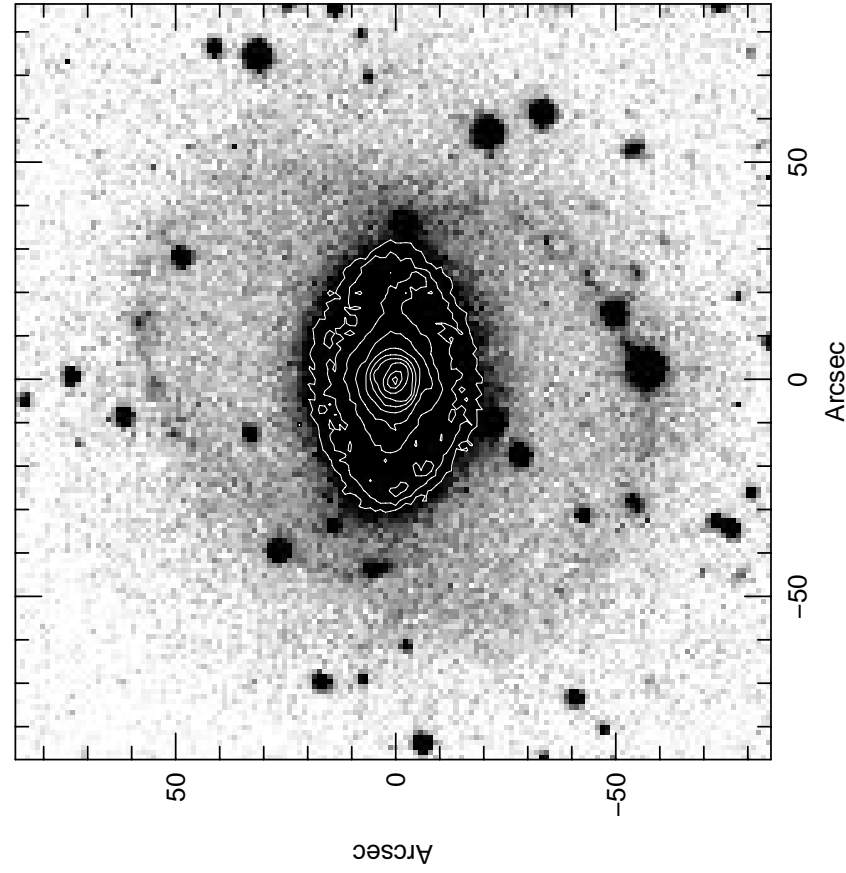


FIG. 1a

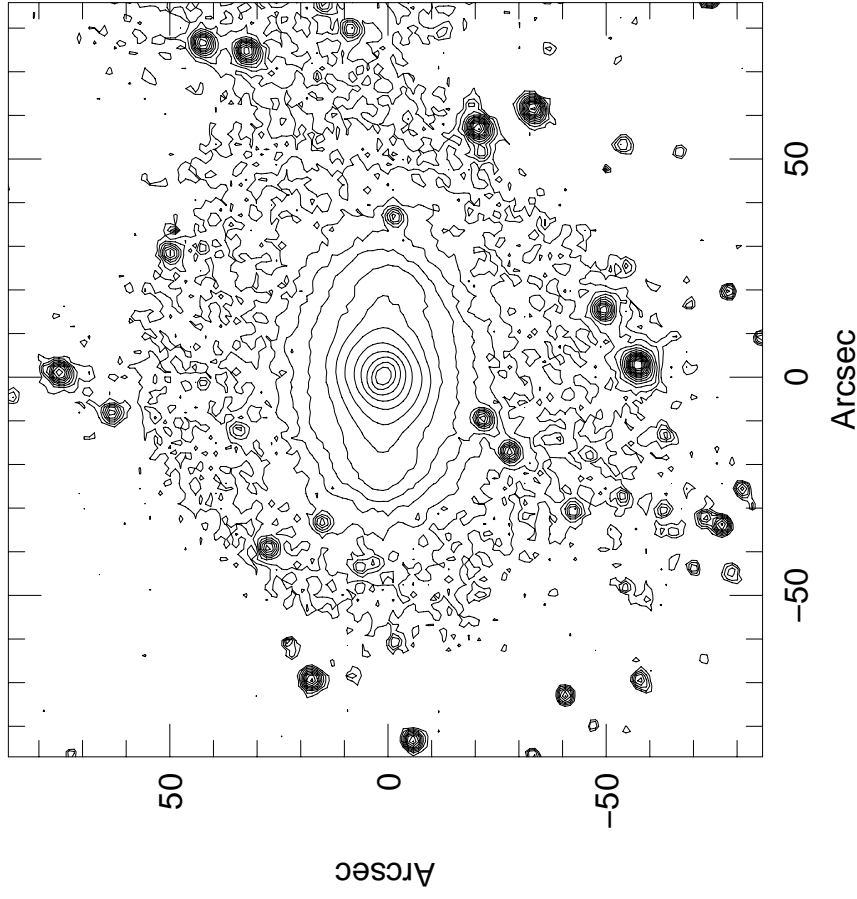


FIG. 1b

FIG. 1.—Images of galaxy NGC 6782. (a) Gray scale B -band image overlaid with contours of the bar 0.5 mag apart. The image is uncalibrated, so we do not know the absolute scale. (b) J -band contours of the bar. The brightest contour is at $15.5 \text{ mag arcsec}^{-2}$, and the difference between contours is $0.5 \text{ mag arcsec}^{-2}$. (c) B/R color map similar to that shown by Buta (1995). (d) Low surface brightness contour in an image that is a noise-weighted sum of the B -, V -, and R -band images. Note the change in angular scale between this figure and the other figures. We note that this outer isophote is almost round, which suggests that the galaxy is not highly inclined.

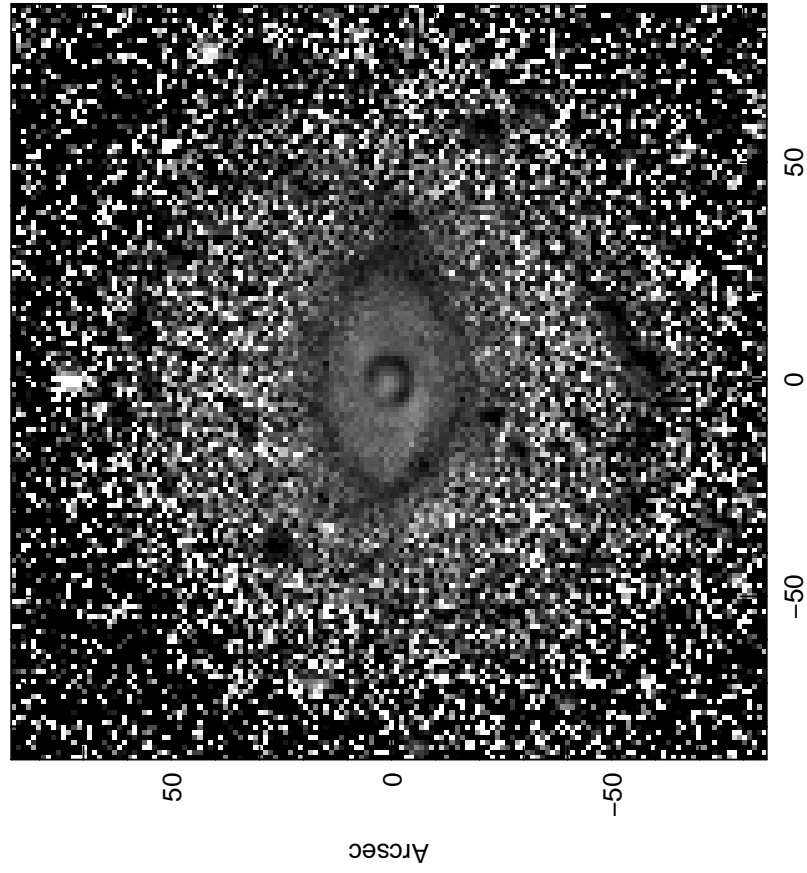


FIG. 1c

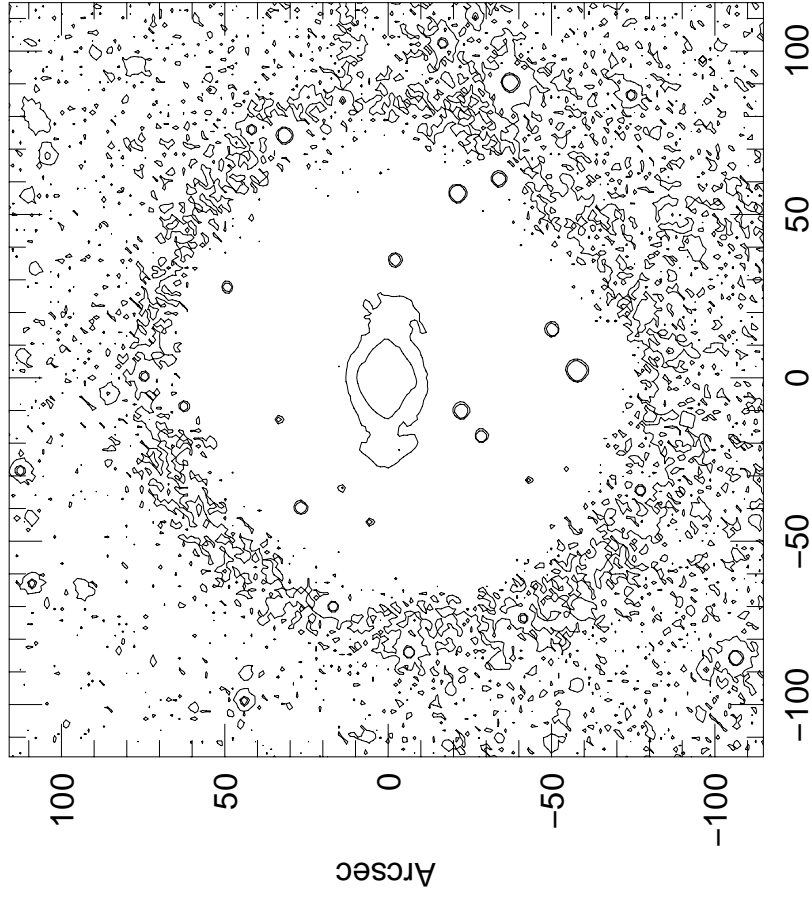


FIG. 1d

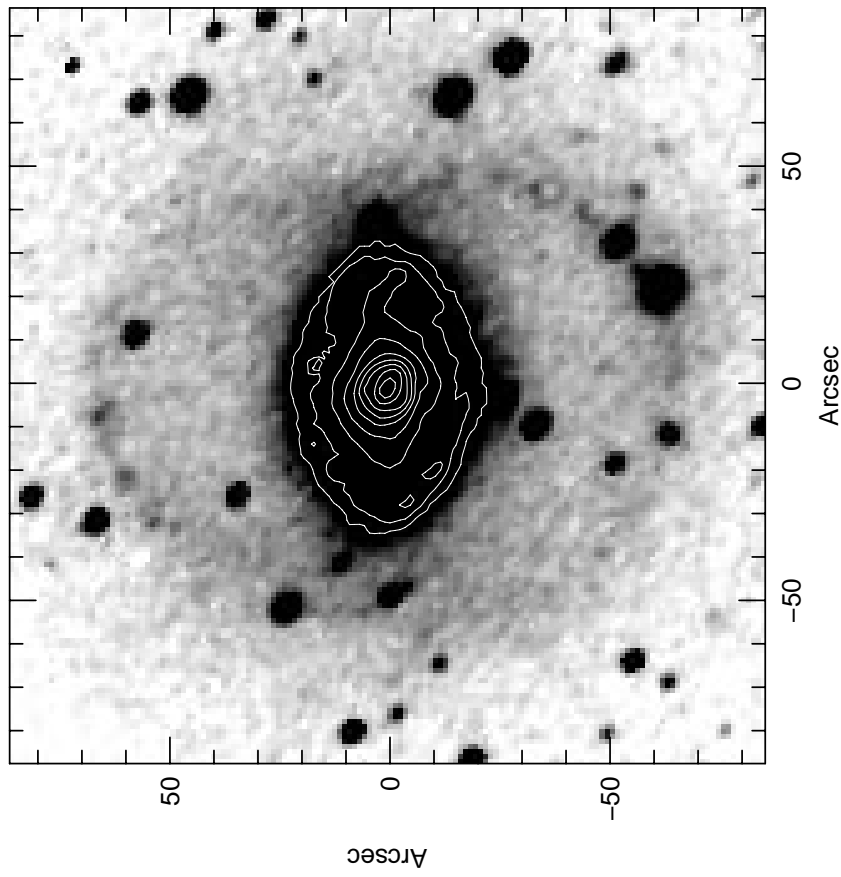


FIG. 2a

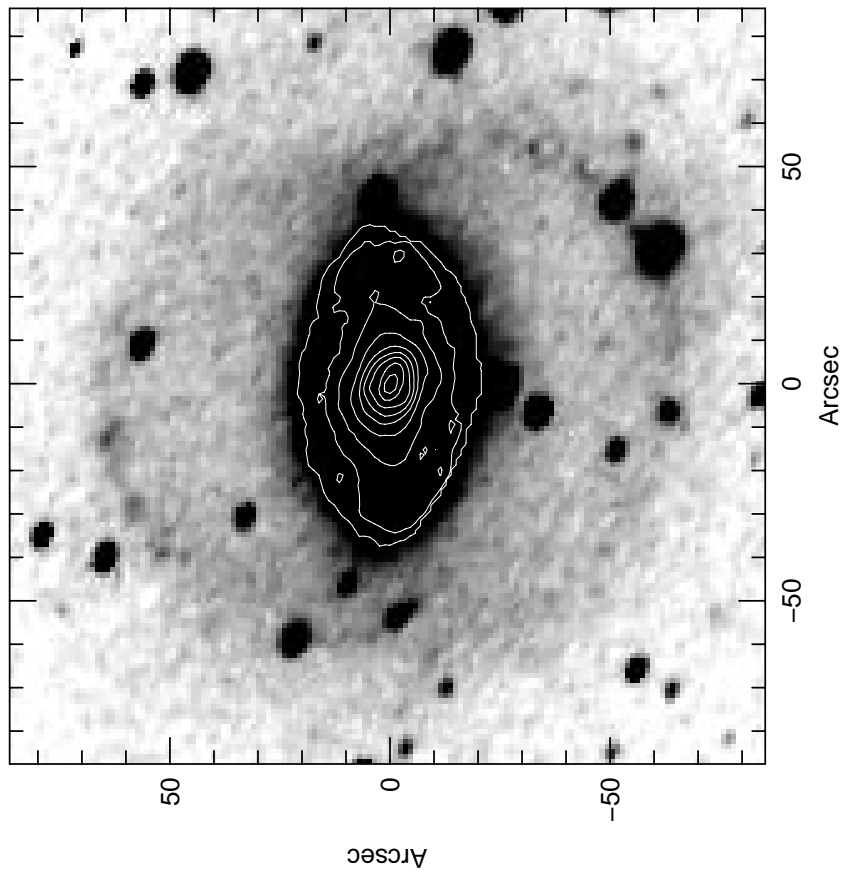


FIG. 2b

FIG. 2.—Face-on, deprojected B -band images of NGC 6782 for the inclinations and position angles listed in Table 1. Note that the higher the galaxy inclination, the rounder the ring and the longer the bar. The position angles have been chosen so that the bar is approximately perpendicular to the ring. These images have been rotated so that the bar has a major axis at $PA \approx 90^\circ$, which is the same as that observed in the original image. (a) $i = 35^\circ$. (b) $i = 41^\circ$. (c) $i = 45^\circ$. (d) $i = 49^\circ$.

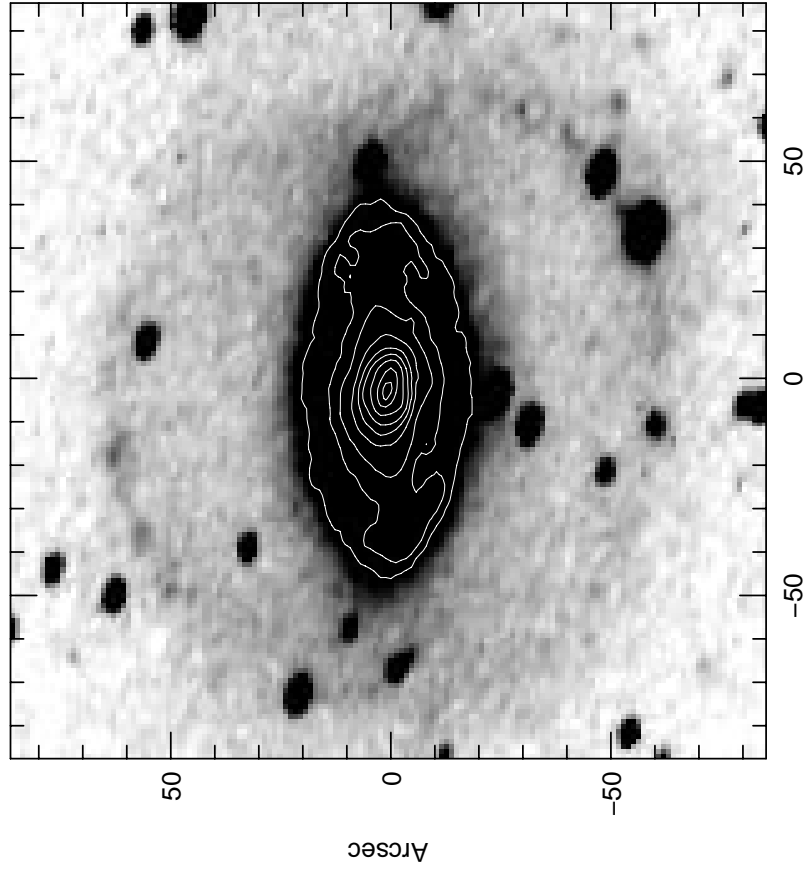


FIG. 2d

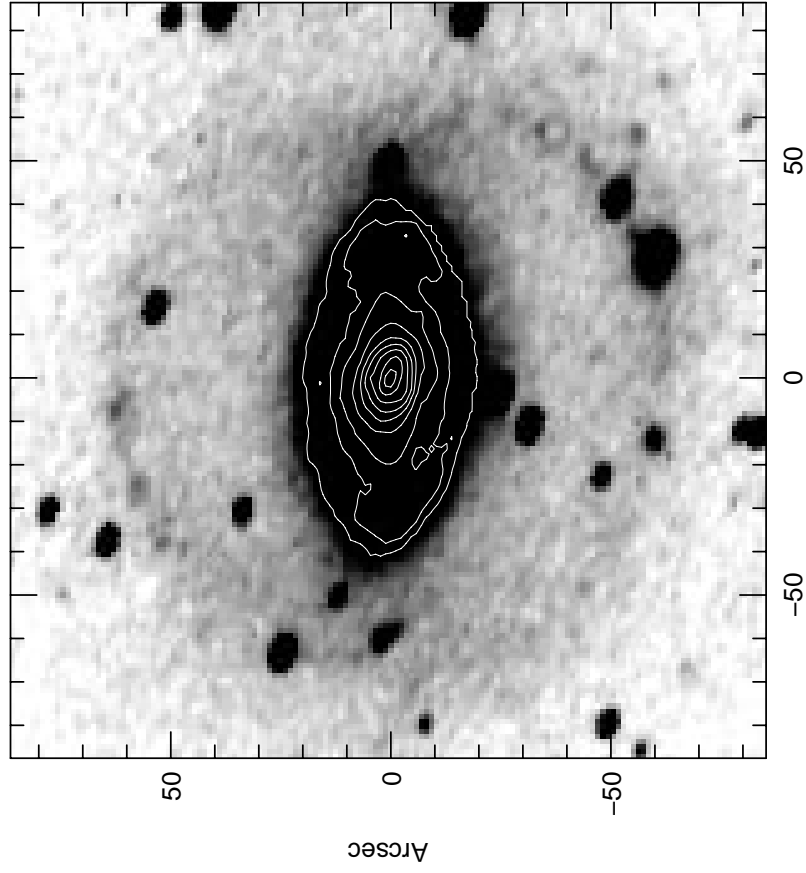


FIG. 2c

TABLE 1
GALAXY ORIENTATION AND EXPONENTIAL FITS TO Φ_2

Inclination (deg)	P.A. (deg) ^a	A (km s ⁻¹) ^{2 b}	a (arcsec) ^c	Outer Axis Ratio ^d
35	-58	3.78×10^4	17.5	1.0
41	-45	3.51×10^4	22.5	0.83
45	-32	3.63×10^4	24.3	0.76
49	-25	3.40×10^4	26.3	0.70

^a Galaxy major axis position angle required for the bar to be perpendicular to the ring at the given inclination.

^b For a maximal disk mass-to-light ratio (see eq. [2]). Once the true circular velocity, v_c , of the galaxy is known, these numbers should be multiplied by $(v_c/320 \text{ km s}^{-1})^2$.

^c Exponential scale length of Φ_2 (see eq. [2]).

^d Axis ratio of the deprojected outer isophote shown in Fig. 1*d*.

so that the major axis position angle is fixed by a choice for the inclination of the galaxy.

Another constraint on the galaxy inclination is obtained from the outermost detected isophotes. We constructed a sum of the B , V , and R images weighted inversely by the noise in each band so as to maximize the signal-to-noise ratio in the outer regions of the galaxy. An outer isophote is displayed in Figure 1*d*; it has a major axis oriented at a position angle of $\sim -45^\circ$ and an axis ratio of ~ 0.9 . This suggests that the galaxy is not highly inclined. Since early-type galaxies are less often warped than late-type galaxies (Bosma 1991), it is unlikely that the galaxy is warped at large radii. We therefore corrected for the inclination, i (where a face-on galaxy has $i = 0^\circ$), of the galaxy using various inclinations and their accompanying position angles (see Table 1). Deprojected images of the galaxies at these inclinations are shown in Figure 2.

The inclination $i = 41^\circ$ causes the ring in the plane of the galaxy to be rounder or to have a larger axis ratio than for $i = 35^\circ$. Inclinations higher than 45° cause the outer isophotes of the galaxy (see Fig. 1*d*) to be very elliptical, or have an axis ratio smaller than 0.8 (see Table 1 for axis ratios). These outer isophotes are not aligned with any feature in the galaxy, so they should be close to circular. Inclinations higher than 45° also cause the ring either to be aligned parallel to the bar or to be almost round (for $i = 49^\circ$, the ring axis ratio is ~ 1.0). This would be inconsistent with the statistics of R1' rings compiled by Buta (1995). For inclinations lower than 35° , the bar and the ring cannot be perpendicular. It is therefore unlikely that the inclination of the galaxy is outside the range $35^\circ < i < 45^\circ$.

After correcting for inclination, the gravitational potential in the plane of the galaxy traced by the luminous stellar matter was determined by convolving the J image of NGC 6782 with a function that depends on the vertical structure of the disk (Quillen et al. 1994). Before convolution, stars were removed from the J image. The disk is assumed to have density $\propto \text{sech}(z/h)$ (following van der Kruit 1988), where z is the height above the plane of the galaxy and h is the vertical scale height. The resulting potential is insensitive to the choice of vertical function for functions such as sech , sech^2 , and exponential with equivalent $\langle z^2 \rangle$ (Quillen 1996a). Since the galaxy is distant, a small vertical scale height was used ($h = 0''.5$). Quillen (1996a) found that doubling the vertical scale height results in raising the Φ_2 component of the gravitational potential by $\sim 10\%$. We have deliberately made h small because the seeing in the images

causes artificial smoothing equivalent to increasing the size of h .

3.3. What Do We Mean by a Maximal Disk?

Figure 3 shows the rotation curve derived from the axisymmetric component of the potential generated from the J image for the different galaxy inclinations. The horizontal line shown in Figure 3 is the circular rotational velocity computed using the Tully-Fisher relation. For an H -band total magnitude of 8.87 measured from our H -band image, we compute a circular velocity of 320 km s^{-1} using the relation given in Pierce & Tully (1992). (All subsequent values given in this paper will be in units with respect to this circular velocity.) This circular velocity is also what we used for the flat rotation curve axisymmetric component of the potential in our orbit integrations at the location of the ring. The rotation curves shown in Figure 3 assume a distance of 50 Mpc ($H_0 = 75 \text{ km s}^{-1} \text{ Mpc}^{-1}$) to the galaxy and a mass-to-light ratio of $M/L_J = 1.23(v_c/320 \text{ km s}^{-1})^2(50$

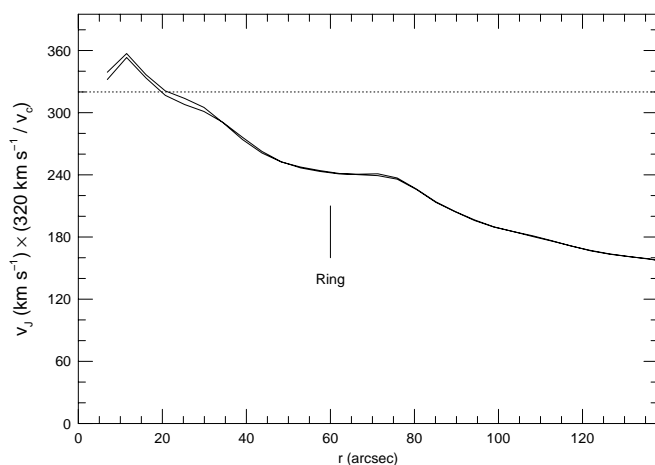


FIG. 3.—Rotation curves from the axisymmetric component of the J -band-generated gravitational potential using the mass-to-light ratio described in the text as “maximal disk.” Rotation curves for galaxy inclinations of $i = 35^\circ$ and 45° have been plotted as solid lines. There is little difference between them. The horizontal, dotted line represents a flat rotation curve with a circular velocity of 320 km s^{-1} predicted using the Tully-Fisher relation. Once the true circular velocity, v_c , of the galaxy is observed, the mass-to-light ratio for the maximal disk should be rescaled. For a nonmaximal disk, the rotation curve resulting from the luminous stellar matter would be lower than that shown here.

Mpc/D) or, using the color of the bar, $M/L_K = 0.69(v_c/320 \text{ km s}^{-1})^2(50 \text{ Mpc/D})$ in solar units (see Worthey 1994), where L_J and L_K are the luminosities in the J and K bands and v_c is the true (not yet measured) circular velocity of the galaxy.

For a maximal disk, the rotation curve is attributed as much as possible to be from the visible components, so that the halo could have a hollow core. (Some authors call a maximal disk solution one with a smooth halo that extends into the nucleus of the galaxy.) The mass-to-light ratio listed above for the disk is what we take to give a maximal disk. This mass-to-light ratio was chosen so that the rotation curve generated from the J -band light reaches above the circular velocity predicted from the Tully-Fisher relation. Once the true circular velocity for the galaxy has been observed, the mass-to-light ratio for the maximal disk can be rescaled. Because the three-dimensional nature of the bulge was not properly taken into account in estimating the potential, the rotation curve is higher (by 10%–20%) than it should be in the central 0"–20". This is why we have chosen the mass-to-light ratio such that the rotation curve is somewhat higher than the circular velocity near the galaxy nucleus (see Fig. 3).

We note that the rotation curve generated from the light drops with increasing radius. At the radius of the ring ($\sim 60''$ – $70''$ or 15–17 kpc), a significant fraction of the mass must be from dark matter. Matter outside of our image that we do not detect exerts a radial force outward, so that the rotation curve predicted from starlight should be even lower at large radii than we show in Figure 3.

3.4. The Nonaxisymmetric Component of the Gravitational Potential

The nonaxisymmetric component of the potential should be due solely to the bar of the galaxy. Since the bar is in the disk of the galaxy, our inaccurate treatment of the bulge of the galaxy does not affect our measurement for $\Phi_2(r)$ (defined in eq. [1]). If luminous matter outside the image is axisymmetric, then once again, our estimate for $\Phi_2(r)$ is not affected by neglecting this matter. This means that our orbit integrations, which use only the Φ_2 component derived from the luminous matter, are not affected by our inaccurate treatment of the bulge and outer disk. Higher order Fourier components of the potential are neglected, since at the ring they are negligible.

The magnitude of the Φ_2 component measured from the potential due to luminous matter is shown in Figure 4 for the various inclinations assumed and for the maximal disk mass-to-light ratio discussed above. The Φ_2 component drops off quickly with radius, as expected for a quadrupolar potential term. An exponential function

$$\Phi_2(r) = A \exp(-r/a) \quad (2)$$

was fitted to these Φ_2 components and is also shown in Figure 4. The numerical values for these fits are listed in Table 1. These numbers show the strength of the nonaxisymmetric component of the potential from the bar for the maximal disk (which correspond to the rotation curves shown in Fig. 3). For the higher inclinations, the Φ_2 component is substantially stronger because the bar becomes longer once deprojected. The exponential scale length of Φ_2 , a , is also larger for the higher inclination case (see Table 1). In the next section, we discuss the effect of changing the disk

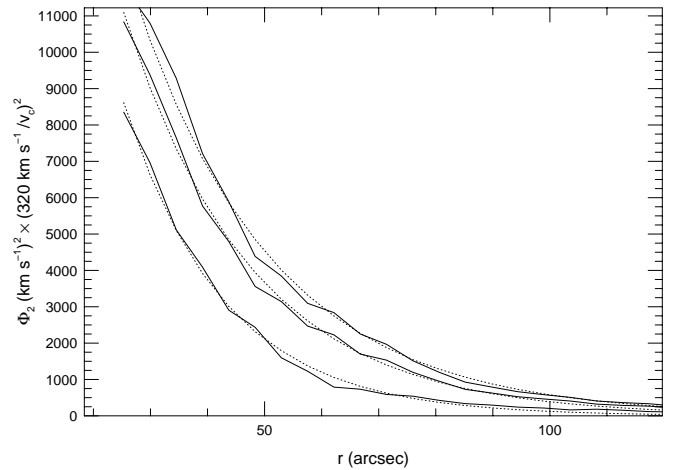


FIG. 4.—Amplitude of the nonaxisymmetric component Φ_2 from the bar of the J -band-generated gravitational potential for the maximal disk. The solid lines are for galaxy inclinations of $i = 45^\circ$, 41° , and 35° , in order of decreasing height. Once the true circular velocity, v_c , of the galaxy is observed, the mass-to-light ratio for the maximal disk should be rescaled. The dotted lines are exponential fits to these curves with strengths and scale lengths listed in Table 1. For the lower galaxy inclinations, Φ_2 is substantially weaker.

mass-to-light ratio (and so the bar strength) on the morphology of the R1' ring.

4. MODELING THE RING

We integrate orbits in the plane of the galaxy for a gravitational potential with an axisymmetric component consistent with a flat rotation curve and circular velocity determined from the Tully-Fisher relation. The nonaxisymmetric component of the potential is derived from exponential fits to the Φ_2 components generated from the J -band image for the various galaxy inclinations assumed. In our integrations, we vary the strength of the bar by adjusting the mass-to-light ratio of the J -band image and by keeping the circular velocity fixed. What we call the maximal disk corresponds to the mass-to-light ratios for the rotation curves shown in Figure 3 and the Φ_2 components shown in Figure 4 with fitting parameters listed in Table 1. Varying the mass-to-light ratio of the disk corresponds to multiplying Φ_2 by a constant that is less than 1. Since the maximal disk mass-to-light ratio is determined by our assumption for the circular velocity (see discussion above), our results are not affected by the fact that actual circular rotational velocity is not known. Periodic orbits (or orbits that are closed in the frame in which the bar is stationary) in the plane of NGC 6782 were found by numerical integration (as in Quillen et al. 1994).

In Figure 5 we show periodic orbits near the outer Lindblad resonance for the maximal disk for a galaxy inclination of 41° . We see that the inner periodic orbits are more pinched near the bar and have a rounder appearance. The outer orbits are more elongated and less pinched near the bar. Points in Figure 5 (and subsequent figures) are shown at equal time steps along the orbit so that the gas density in the orbit should be high in the pinches near the bar. Correspondingly, the speed of the gas decreases in the pinches. Measurement of the velocity field in the ring should constrain the degree of cuspsiness of the orbits. As pointed out

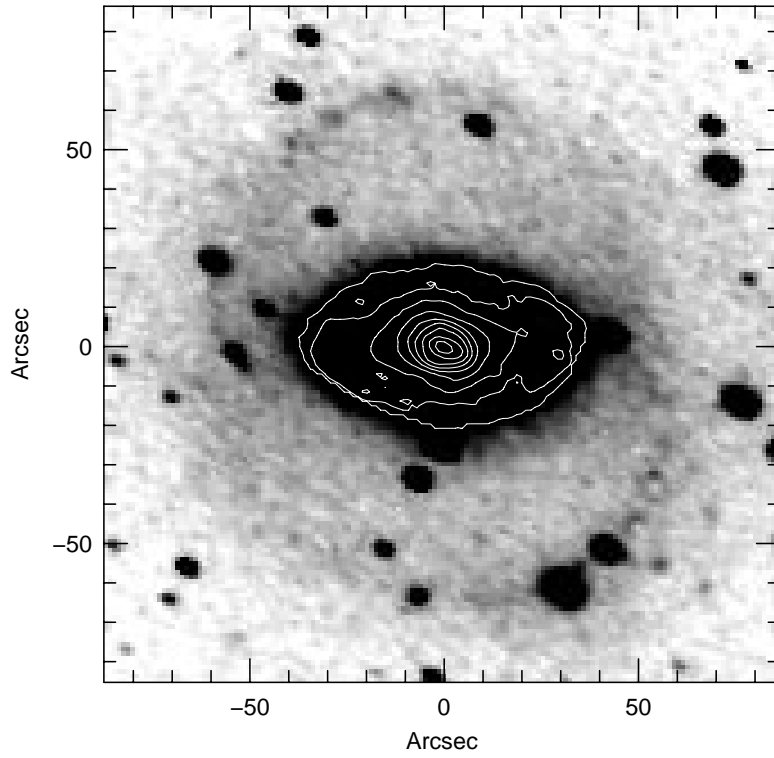


FIG. 5a

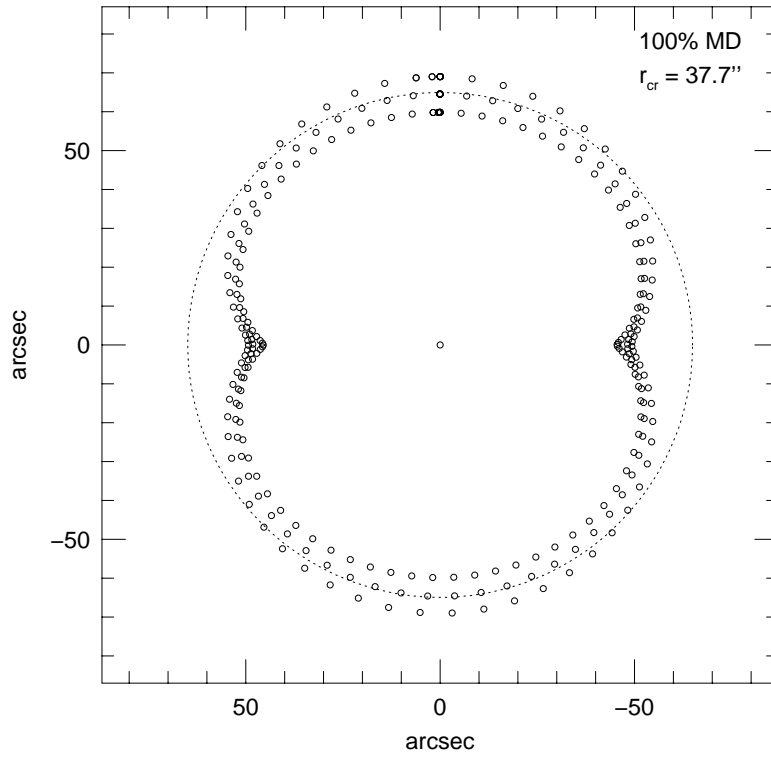


FIG. 5b

FIG. 5.—Comparison of periodic orbits with the morphology of the ring at a galaxy inclination of $i = 41^\circ$. (a) Gray scale of the deprojected galaxy NGC 6782, face-on. (b) Periodic orbits near the outer Lindblad resonance. The mass-to-light ratio of the bar in units of percent of the maximal disk value (MD) and the corotation radius (r_{cr}) are printed in the upper right-hand corner of the plot. Points are plotted at equal time steps in the rotating frame in which the bar is still. Note that speeds are slower in the pinches near the bar ends. The dotted circle shows the location of the outer Lindblad resonance. The maximal disk provides a good representation for the morphology of the ring.

by Kalnajs (1991), the gas in the ring cannot be in an orbit that intersects itself or that has loops. We therefore consider only orbits that are not self-intersecting. For the orbits shown in Figure 5a, the radius of corotation is $37''.7$ and the bar angular rotation rate or pattern speed is $(35.0 \text{ Gyr}^{-1}) \times (v_c/320 \text{ km s}^{-1})(50 \text{ Mpc}/D)$. For our rotation curve, this pattern speed places the radius of corotation just past the end of the bar, as predicted theoretically and inferred from observations of bars. Figure 5 shows that the maximal disk

provides a good fit to the morphology of the ring for a galaxy inclination of $i = 41^\circ$. In the following sections, we explore the sensitivity of the ring morphology to the bar strength, the bar pattern speed, and the galaxy inclination.

4.1. Varying the Strength and Pattern Speed of the Bar

Figure 6 shows comparisons between periodic orbits with the same apogee for different bar strengths and pattern speeds at a galaxy inclination of $i = 41^\circ$. All figures compare

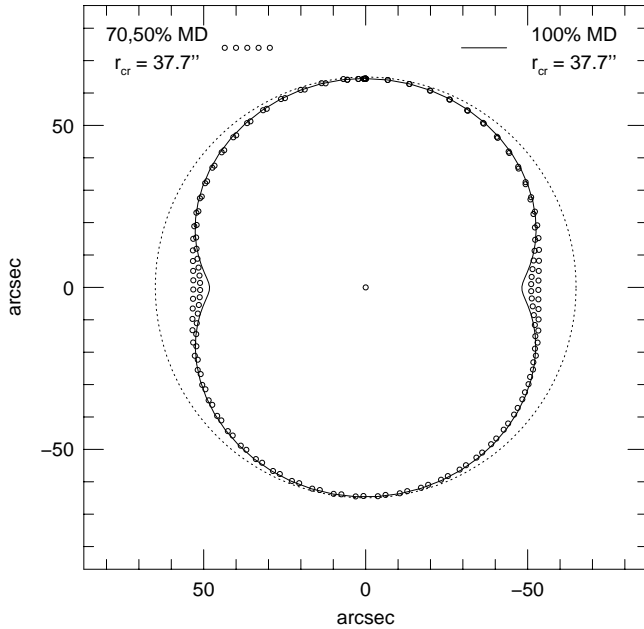


FIG. 6a

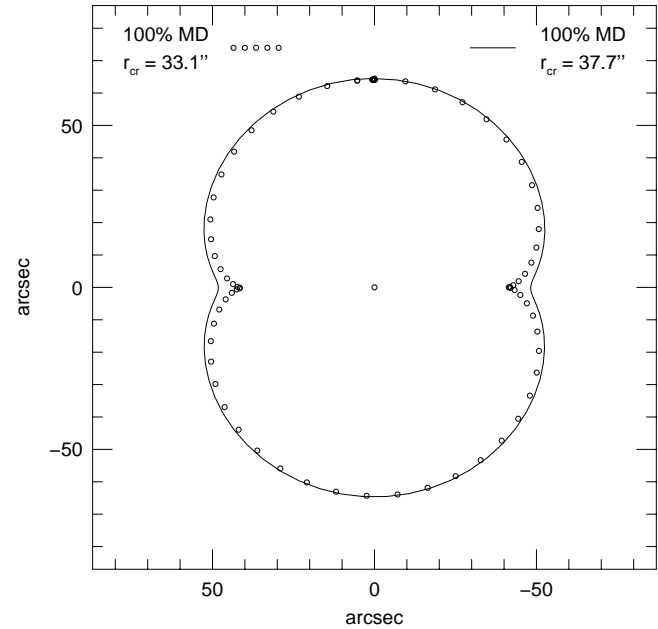


FIG. 6b

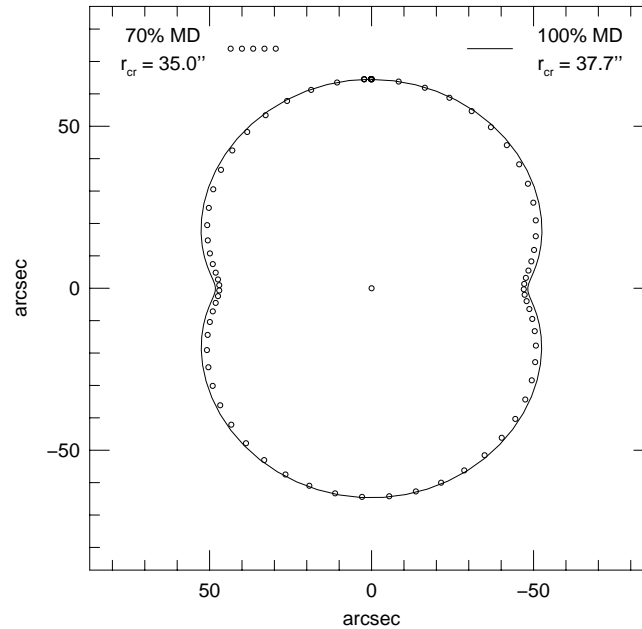


FIG. 6c

FIG. 6.—(a) Effect of varying the bar strength on the shape of the orbits with the same apogee for a galaxy inclination $i = 41^\circ$. A periodic orbit for the maximal disk (solid line) compared to a similar orbit for weaker bars with mass-to-light ratios that are 70% and 50% as large as the maximal disk value (open circles). These orbits are derived from bars with the same corotation radii. The dotted circle shows the location of the outer Lindblad resonance. Bar strengths, in units of percent of the maximal disk value (MD), and the corotation radii (r_{cr}) are printed in the upper right-hand corners of the plots. (b) The effect of varying the bar pattern speed on the shape of the orbits with the same apogee. A periodic orbit for the maximal disk (solid line) compared to a similar orbit with the same bar mass-to-light ratio but a faster bar. (c) By increasing the speed and decreasing the strength of the bar differences in the orbit shapes can be minimized. A pinched non-self-intersecting orbit for the maximal disk (solid line) compared to a similar orbit (open circles) for a faster and weaker bar.

an orbit shown in Figure 5a that has a maximal disk mass-to-light ratio with a similar orbit for either lower bar mass-to-light (Fig. 6a), faster bar (Fig. 6b), or both (Fig. 6c). Figure 6a shows the comparison for two bars with the same pattern speed. We note that the weaker bars have rounder, less pinched orbits of the same apogee. Figure 6b shows a comparison between a slow and a faster bar with the same bar strengths. We can see that the faster bar has a more elongated and strongly pinched orbit of the same apogee. In Figure 6c, we can see that by decreasing the bar strength and increasing the bar pattern speed, differences in the shapes of orbits with the same apogee can be minimized.

Weakening the bar potential at the location of the ring (equivalent to decreasing the disk mass-to-light ratio) to less than 70% of the maximal disk value causes the pinched orbits to be rounder and less pinched than the observed ring. We find that it is not possible to consistently match the morphology of the ring by raising the bar pattern speed in a weaker bar, since this decreases the radius of corotation to within the bar ends. For the orbits shown in Figure 5 (and the solid line in Fig. 6a, 6b, and 6c), the corotation radius lies just outside the end of the bar at a radius of $37''.7$. The faster bar (with its corresponding orbit shown as open circles in Fig. 6c) that would fit the ring morphology places the radius of corotation at $33''.1$, which lies within the end of the bar—a situation that is not thought to be theoretically possible (Contopoulos et al. 1989). As a result, we find that for an assumed inclination of $i = 41^\circ$, the bar mass-to-light ratio must be greater than 70% of the maximal disk value.

4.2. Changing the Galaxy Inclination

For a lower galaxy inclination of $i = 35^\circ$, the strength of the Φ_2 component is about half as large of that with $i = 41^\circ$ at the location of the ring (see Fig. 4). As expected from the previous section, it is not possible to match the ring morphology with the periodic orbits without increasing the mass-to-light ratio past what we have defined as the maximal disk value or decreasing the radius of corotation to a radius smaller than the bar length. Figure 7 shows orbits integrated for a maximal disk mass-to-light ratio with a bar corotation radius of $32''.2$. Orbits with larger apogees than that shown in Figure 7 become self-intersecting with small loops at their minor axes and are probably unstable. The non-self-intersecting periodic orbits are too round to match the observed ring morphology. It is not possible to resolve the problem by raising the bar angular rotation rate, since this would place the radius of corotation within the end of the bar.

It would be possible to have a stronger bar or a larger mass-to-light ratio with a more carefully estimated maximal disk value at $i = 35^\circ$. For example, if the rotation curve of the galaxy decreases with radius near the ring, then the maximal disk value for the mass-to-light ratio could be higher. The ring enveloping the bar that is quite blue (see Fig. 1c) may contain a large gas mass. Including this gas mass increases the strength of the nonaxisymmetric component (Φ_2) of the potential and so causes the periodic orbits near the outer Lindblad resonance to be more elongated. In short, we find that for an assumed inclination of $i = 35^\circ$, the bar mass-to-light ratio must be greater than the maximal disk value assumed here.

For higher galaxy inclinations, the outer ring becomes rounder and the bar lengthens (see Fig. 2). A mass-to-light ratio lower than the maximal disk value is required to

match the observed morphology of the ring. In Figure 8, we show periodic orbits for a galaxy inclination of 45° that resemble the morphology of the ring for a mass-to-light ratio that is 75% of the maximal disk value. Since the average radius of the ring is larger for this galaxy inclination than for lower inclinations, the bar angular rotation rate must be lower. Mass-to-light ratios lower than 60% again cause the ring to be too round to match the morphology of the ring. Mass-to-light ratios higher than 90% eliminated the R1 periodic orbits (the resonance was very strong) at the radius of the ring for pattern speeds that kept the corotation radius outside the bar ends. As a result, we find that for an assumed inclination of $i = 45^\circ$, the bar mass-to-light ratio must be within $75\% \pm 15\%$ of the maximal disk value.

It is extremely unlikely that the galaxy inclination is much higher than 45° , since at 50° the ring is almost round and the outer isophotes of the galaxy are even more elongated (see Fig. 2).

5. SUMMARY

5.1. Underlying Assumptions

We have assumed the following in modeling the R1' outer ring in NGC 6782:

1. The ring morphology consists of gas in periodic non-self-intersecting orbits near the outer Lindblad resonance, and spiral structure in the ring does not cause the morphology to deviate significantly from these periodic orbits.
2. The bar is perpendicular to the ring. This allowed us to determine the position angle for a given galaxy inclination.
3. The rotation curve is flat.
4. The Φ_2 nonaxisymmetric component of the potential is only due to the bar as seen in the *J*-band image (gas is neglected) and does not twist (eq. [1]).
5. The maximal disk mass-to-light ratio is well estimated from the axisymmetric component of the *J*-band-generated potential.

Many of these assumptions can be constrained with a velocity field that can determine the inclination and measure the rotation curve of the galaxy. However, the first assumption listed above is of particular concern. Strong spiral structure in the ring will cause the gas to deviate from the periodic orbit families explored here. While it is not unreasonable to expect that the gas is close to the periodic orbits (in the same way gas in the Milky Way is primarily undergoing circular motion despite its spiral structure), future work should both study R1 ring galaxies with minimal spiral structure and investigate the role of the spiral structure in these rings.

5.2. Discussion

In this paper we have explored the shape of the periodic orbits near the outer Lindblad resonance in a ring galaxy using a nonaxisymmetric gravitational potential based upon a near-infrared image of the bar. We find that the shape of the non-self-intersecting periodic orbits at the outer Lindblad resonance is affected by the strength of the nonaxisymmetric component Φ_2 of the gravitational potential. A stronger bar (corresponding to a larger Φ_2) or a faster bar result in more elongated orbits at the radius of the ring.

Using the assumptions listed above and comparing outer ring morphology of NGC 6782 with the integrated non-

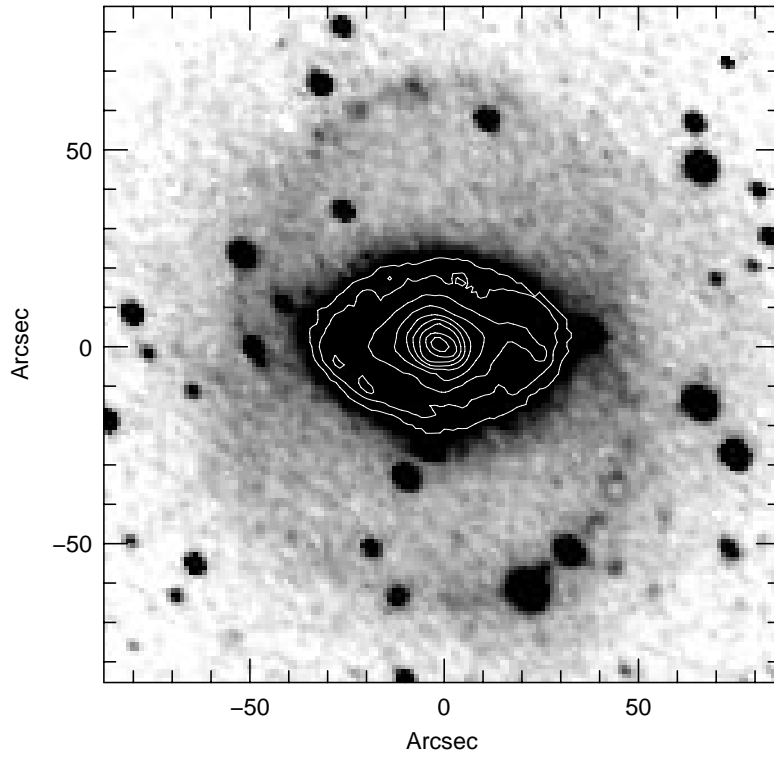


FIG. 7a

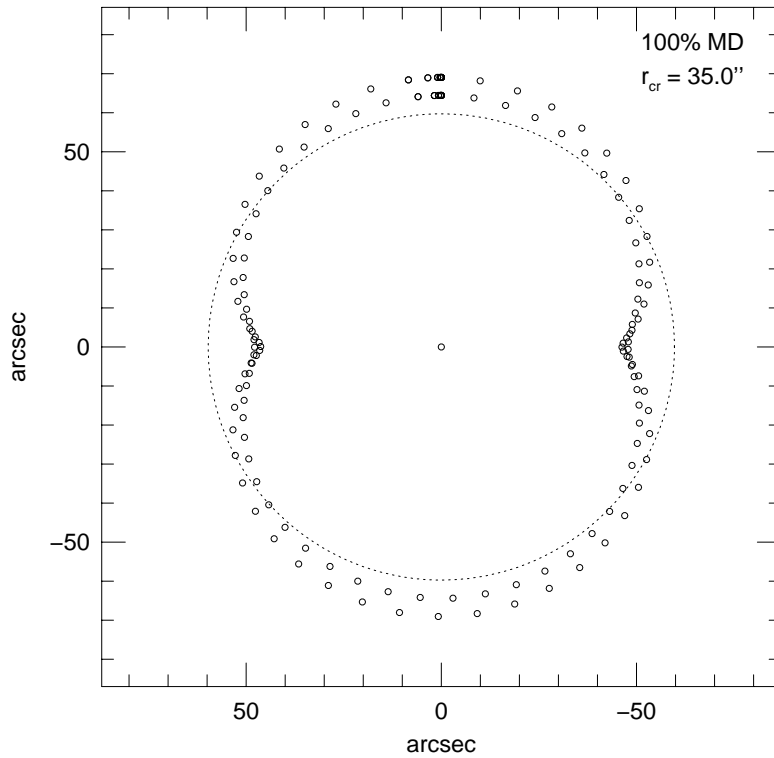


FIG. 7b

FIG. 7.—Comparison of periodic orbits with the morphology of the ring at a galaxy inclination of $i = 35^\circ$. (a) Gray scale of the deprojected galaxy NGC 6782, face-on. (b) Periodic orbits near the outer Lindblad resonance. The mass-to-light ratio of the bar in units of percent of the maximal disk value (MD) and the corotation radius (r_{cr}) are printed in the upper right-hand corner of the plot. Points are plotted at equal time steps in the rotating frame in which the bar is still. The dotted circle shows the location of the outer Lindblad resonance. The maximal disk value for the mass-to-light ratio produces non-self-intersecting orbits that are insufficiently elongated to be consistent with the morphology of the ring.

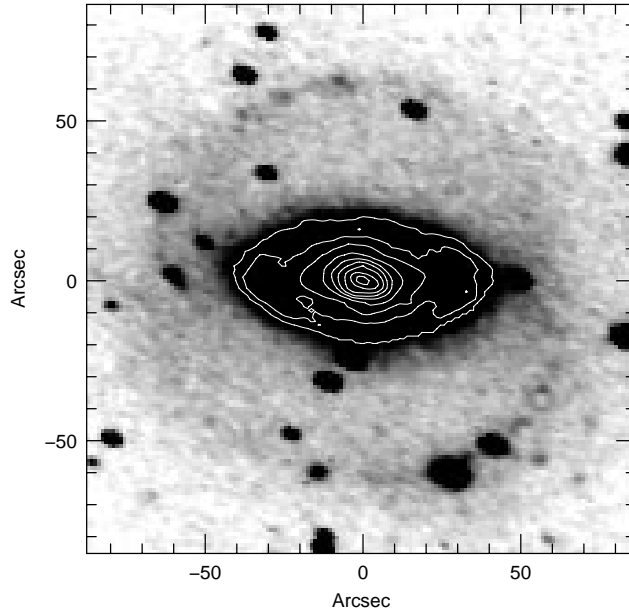


FIG. 8a

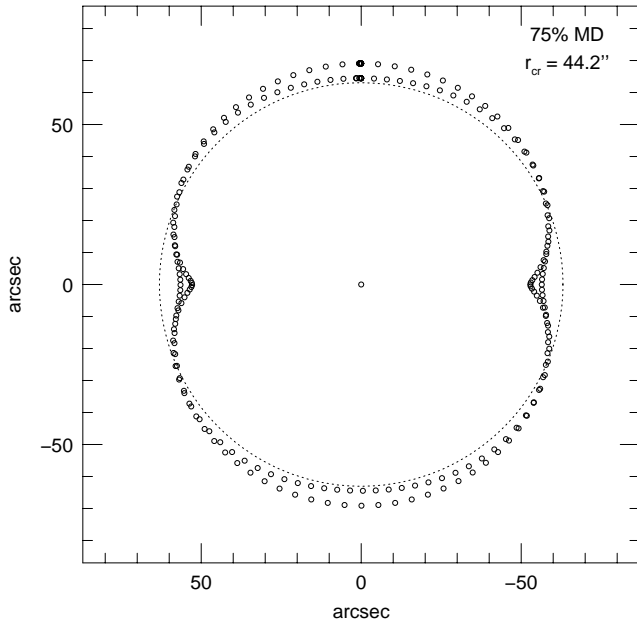


FIG. 8b

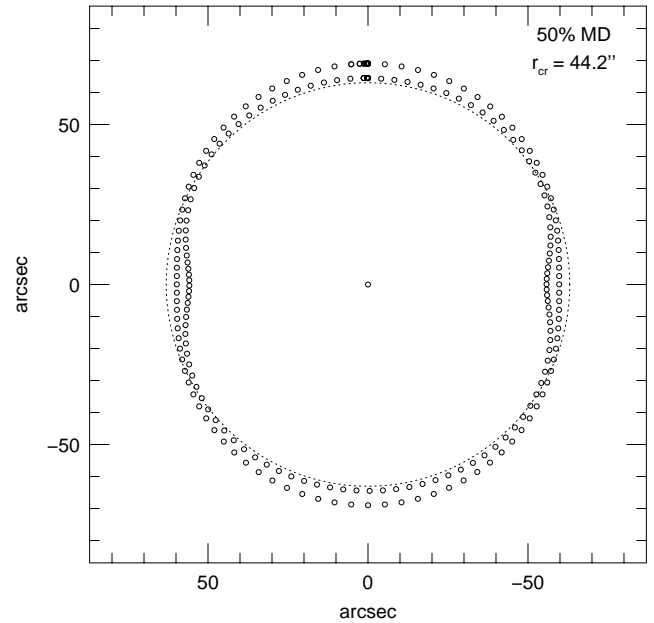


FIG. 8c

FIG. 8.—Comparison of periodic orbits with the morphology of the ring at a galaxy inclination of $i = 45^\circ$. (a) Gray scale of the deprojected galaxy NGC 6782, face-on. (b) Periodic orbits near the outer Lindblad resonance. The mass-to-light ratio of the bar in units of percent of the maximal disk value (MD) and the corotation radius (r_{cr}) are printed in the right-hand corner of the plot. Points are plotted at equal time steps in the rotating frame in which the bar is still. The dotted circle shows the location of the outer Lindblad resonance. The mass-to-light ratio of 75% of the maximal disk value provides a good representation for the morphology of the ring. (c) Same as (b) but with a weaker bar.

self-intersecting periodic orbits, we find that the bar mass-to-light ratio can be constrained given an assumed galaxy inclination. For a galaxy inclination of 41° , we find that a bar mass-to-light ratio greater than 70% of the maximal disk value is needed to match the ring morphology. It is not possible to match the morphology of the ring with a weaker and faster bar, since this places the bar corotation radius within the end of the bar. For $i = 45^\circ$, we find a mass-to-light ratio of $75\% \pm 15\%$ of the maximal disk value matches the morphology of the ring. For $i = 35^\circ$, a value

larger than the maximal disk value assumed here is required. A larger mass-to-light ratio could be allowed if a large gas mass is found in the ring enveloping the bar (increasing the Φ_2 component of the potential), or if the rotation curve decreases near the ring.

Larger galaxy inclinations are unlikely for the following reasons: (1) The ring becomes round or aligned with the bar that is not supported by statistics of R1-type rings (Buta 1995). However, NGC 6782 could be a special case. (2) The outer isophotes of the galaxy become significantly elon-

gated. Deeper images showing the shapes of the isophotes past the ring may help to constrain the inclination angle of the galaxy.

We note that here that the method considered here places a constraint on the strength of the nonaxisymmetric ($m = 2$) component of the potential from the bar. Since the bar is necessarily a disk component, this leads directly to a constraint on the disk mass-to-light ratio. Once the rotation curve is observed, the morphology of the ring gives a constraint on the disk mass-to-light ratio that is independent of any assumptions about the halo or dark matter distribution. As a result, a measured rotation curve would allow us to measure the core radius of the dark matter halo using our values for the mass-to-light ratio. A measured rotation curve will also enable us to place a value on the maximal disk mass-to-light ratio assumed here and check whether our assumption of a flat rotation curve is a good one.

Modeling an observed velocity field in the ring will make it possible to measure the mass-to-light ratio of the bar with more precision than with a purely morphological comparison as done here. Velocities observed along the major axis of the ring should constrain the inclination of the galaxy. Highly pinched orbits have slow speeds in their pinches, as inferred from the small spacing in the equal time step points shown in Figures 5–8. The velocity field should also therefore limit which particular orbits are represented in the ring. The asymmetry of the velocity field will also constrain the degree of deviation from the periodic orbits caused by spiral structure in the ring.

We also plan to observe other ring galaxies to find if high

mass-to-light ratios are required generally. Modeling of galaxies with different orientations should help resolve the uncertainties caused by projection.

Gas simulations of rings could be studied to discover how well closed orbits match the gas morphology in these systems, which particular orbits collect gas, and how close outer rings are to being perpendicular to their bars. The effect of spiral structure on the morphology of the ring should also be studied.

If a near-maximal disk value for the bar mass-to-light ratio is indeed required (as suggested here), then either the inner parts of galaxies have little dark matter or the dark matter contained in the disk of the galaxy is non-axisymmetric and rotates with the bar. The second possibility implies that the “conspiracy of shapes” suggested by Sackett et al. (1994) extends into the bar and would lend support to the idea that dark matter halos are flattened (Sackett et al. 1994; Olling 1996), since, if the dark matter rotates, it should be flattened.

We acknowledge helpful discussions and correspondence with R. Buta, A. Gould, D. Weinberg, K. Griest, P. Sackett, G. Rieke, and A. Bosma. We thank the referee for helpful comments, which significantly improved the paper. The OSU galaxy survey is being supported in part by NSF grant AST 92-17716. A. C. Q. acknowledges the support of a Columbus fellowship and a grant for visitors from L’Observatoire de Marseille. J. A. F. thanks Roger Davies for his hospitality at Durham University and PPARC for partial support via a Visiting Senior Research Fellowship.

REFERENCES

- Begeman, K. G., Broeils, A. H., & Sanders, R. H. 1991, *MNRAS*, 249, 523
 Bosma, A. 1991, in *Warped Disks and Inclined Rings around Galaxies*, ed. S. Casertano, P. D. Sackett, & F. H. Briggs (Cambridge: Cambridge Univ. Press), 181
 Broeils, A. H., & Courteau, S. 1997, in *ASP Conf. Proc., Dark and Visible Matter in Galaxies and Cosmological Implications*, ed. M. Persic & P. Salucci (San Francisco: ASP), in press
 Buta, R. 1995, *ApJS*, 96, 39
 Buta, R., & Combes, F. 1996, *Fundam. of Cosmic Physics*, 17, 95
 Buta, R., & Crocker, D. A. 1991, *AJ*, 102, 1715
 Buta, R., Lewis, M., & Purcell, G. B. 1997, in preparation
 Byrd, G., Rautiainen, R., Salo, H., Buta, R., & Crocker, D. A. 1994, *AJ*, 108, 476
 Contopoulos, G., Gottesman, S. T., Hunter, J. H., Jr., & England, M. N. 1989, *ApJ*, 343, 608
 Contopoulos, G., & Grosbøl, P. 1989, *A&A Rev.*, 1, 261
 Frogel, J. A. 1988, *ARA&A*, 26, 51
 Frogel, J. A., Quillen, A. C., & Pogge, R. W. 1996, in *New Extragalactic Perspectives in the New South Africa*, ed. D. Block (Dordrecht: Kluwer), 65
 Kent, S. M. 1987a, *AJ*, 91, 1301
 ———. 1987b, *AJ*, 93, 816
 Kalnajs, A. J. 1991, in *Dynamics of Disk Galaxies*, ed. B. Sundelius (Göteborgs, Sweden: Göteborgs Univ. Press), 323
 Olling, R. P. 1996, *AJ*, 112, 481
 Pierce, M. J., & Tully, R. B. 1992, *ApJ*, 387, 47
 Pogge, R. W., et al. 1997, in preparation
 Quillen, A. C. 1996a, in *Spiral Galaxies in the Near-IR*, ed. D. Minniti & H.-W. Rix (Berlin: Springer), 157
 ———. 1996b, preprint (astro-ph/9609041)
 Quillen, A. C., Frogel, J. A., & González, R. A. 1994, *ApJ*, 437, 162
 Quillen, A. C., Frogel, J. A., Kenney, J. D., Pogge, R. W., & DePoy, D. L. 1995, *ApJ*, 441, 549
 Sackett, P. D. 1997a, *PASA*, 14, 11
 ———. 1997b, *ApJ*, 483, 103
 Sackett, P. D., Rix, H.-W., Jarvis, B. J., & Freeman, K. C. 1994, *ApJ*, 436, 629
 Schwarz, M. P. 1981, *ApJ*, 247, 77
 van der Kruit, P. C. 1988, *A&A*, 192, 117
 Worthey, G. 1994, *ApJS*, 95, 107